Carp D-amino acid oxidase: Structural active site basis of its catalytic mechanisms

Mohammed Golam Sarower[a,b,*]**, Shigeru Okada**[a]**, Hiroki Abe**[a,c]

[a] Department of Aquatic Bioscience, Graduate School of Agricultural and Life Sciences, University of Tokyo, Bunkyo, Tokyo 113-8657, Japan

[b] Fisheries and Marine Resource Technology Discipline, Khulna University, Khulna 9208, Bangladesh

[c] Research Institute of Seafood Biochemistry, 3-23-20 Kamiigusa #205, Suginami, Tokyo 167-0023, Japan

*Corresponding author, e-mail: sarower@yahoo.com

ABSTRACT: The three-dimensional structure of the flavoprotein D-amino acid oxidase (DAO, EC 1.4.3.3) from carp hepatopancreas (chDAO) and its active site cavity was modelled using ProModII. The structural features relevant for the overall conformation and for the catalytic activity are described. Secondary structure topology consists of 11 α-helices and 17 β-strands, which differs slightly from pig kidney, and *Rhodotorula gracilis* DAOs. chDAO showed a theoretical 'head-to-head' mode of dimerization. The presence of a short 'lid' in chDAO covering the active site, commonly found in mammalian DAO but absent in *R. gracilis* DAO, is interpreted as the origin of the differences in kinetic mechanism among these enzymes. This lid has been proposed to control the access of the substrate to the active site and to regulate dissociation of products. The conformational change in the large size active site loop determines the overall rate of turnover of DAOs. The shorter active site loop found in chDAO might be responsible for the higher turnover rate in chDAO compared to that of pkDAO.

KEYWORDS: active site, three-dimensional structure, dehydrogenation

INTRODUCTION

It was once generally believed that no D-amino acid of any kind exists in the body of mammals. However, due to the improvement in the detection method of distinguishing enantiomeric amino acids, it has now been established that D-amino acids do occur in various organisms including mammals[1,2]. Moreover, certain D-amino acids play critical roles in regulating neural activities in vivo[3]. In contrast, the D-Amino acid oxidase (DAO, EC 1.4.3.3), a flavin adenine dinucleotide (FAD)-dependent and highly stereoselective flavoenzyme, occurs widely in microorganisms[4–6] and in animal tissues[7–9]. It is a marker enzyme of microbodies in yeast and peroxisomes of higher organisms[10]. Since Krebs[11] discovered DAO in animal tissues, it has served as a subject for enzymological, biophysical, and medical investigations. The primary structure has been reported on the basis of the amino acid and nucleotide sequences of the cDNA[12–14].

In view of the growing interest in the physiological functions of D-amino acids, DAO is also considered important in regulating the levels of D-amino acids related to neural activity[15,16]. Several recent investigations revealed that DAO was respon-
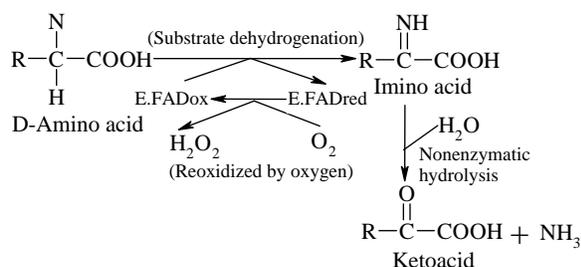
Fig. 1 Scheme showing the principles underlying the oxidative deamination of D-amino acid by D-amino acid oxidase.

sible for metabolizing exogenous and endogenous free D-amino acids in animals[14,17]. DAO catalyses oxidative deamination of a variety of D-amino acids (Fig. 1). When a substrate binds to the active site of the enzyme, it is dehydrogenated to an imino acid by the enzyme-bound FAD in a reduced state. The imino acid then is released from the active site and hydrolysed nonenzymatically to a ketoacid and ammonia. Reduced FAD is reoxidized by molecular oxygen, thereby closing the catalytic cycle.

Despite its long history of enzymological as well

as physico-chemical studies, the detailed molecular events during the catalytic sequence were not totally clear due to the lack of the active-site structure at atomic resolution. Very recently, these molecular details have been solved by X-ray crystallography[18].

We have cloned a gene encoding DAO from the hepatopancreas of carp (*Cyprinus carpio*) for the first time in a non-mammalian species (GenBank accession no. AY421707)[12] and characterized its catalytic and theoretical structural properties[3]. In this paper, we report the structural properties of the carp DAO active site and compare it with those of mammalian and yeast DAOs. We also identify the factors that determine catalytic efficiency and the stability of the dimeric forms of DAO.

MATERIALS AND METHODS

The deduced amino acid sequence of chDAO (Gen-Bank accession no. AY421707) was used as the starting materials for model building[14].

Comparative protein modelling requires at least one sequence of known experimental three-dimensional structure with a significant similarity to the target protein. SWISS-MODEL (http://swissmodel.expasy.org), a server for automated comparative modelling of three-dimensional protein structure, selected three modelling templates of pig kidney DAO (pkDAO, PDB entry code: 1evi, 1an9, and 1aa8) from Brookhaven Protein Data Bank (PDB).

The sequence of chDAO was aligned with the selected templates by the structurally corrected multiple sequence alignment using the best-scoring diagonals obtained by sequence alignment algorithms[19]. A structural alignment was generated after removing incompatible templates, i.e., omitting structures with high C_α root mean square deviations.

The three-dimensional model of chDAO was built with ProModII (SWISS-MODEL), an automated knowledge-based protein-modelling tool[20]. The experimentally determined structural coordinates of DAOs (PDB entry code: 1evi, 1an9, and 1aa8)[18, 21, 22] were used as references for model building. The backbone atom positions of these template structures were averaged. The templates were thereby weighted by their sequence similarity to the chDAO sequence, while significantly deviating atom positions were excluded.

Deviation in the protein structure geometry was regularized by steepest descent and conjugate gradient energy minimization using the GROMOS96 force field[23].

The three-dimensional structure of chDAO was compared with that of pkDAO (PDB entry code: 1kif) and *Rhodotorula gracilis* DAO (RgDAO, PDB entry code:1c0i). The coordinates of the Kamiigusa structures were viewed, analysed, and edited by Swiss-PdbViewer 3.7[24] and protein explorer software.

RESULTS AND DISCUSSION

Overall structure and topology

Structural parameters possibly involved in the catalytic properties of chDAO were examined by tertiary structure modelling. The three-dimensional structure obtained from SWISS-MODEL[20] is depicted in Fig. 2. Secondary structure elements have been adopted and named according to the topology described by Mattevi et al[25]. The chDAO subunit is schematically shown in Fig. 3. Each subunit is clearly divided into two domains, a FAD binding domain with the dinucleotide-binding fold observed
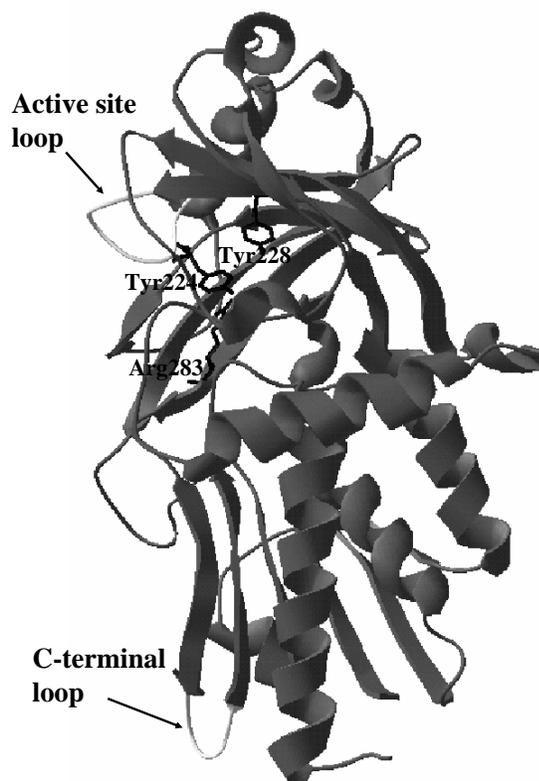
Fig. 2 Ribbon representations of chDAO monomer structure constructed with ProModII. Arg283, Tyr224, and Tyr228 are thought to be key catalytic residues. The letters N and C indicate the N and C terminus of the protein, respectively. The active site loop contains residues 218-226 and C-terminal loop contains residues 297–302.
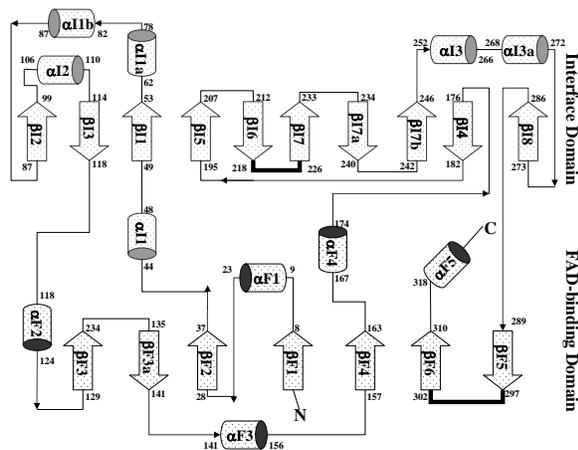
Fig. 3 Secondary structure topology of DAO according to Mattevi et al[25]. Cylinders: α-helices; arrows: β-strands. The secondary structure elements of the interface domain and FAD-binding domain are labelled by the letters I and F, respectively, followed by the sequential number.

in several flavoenzymes[26], and an interface domain. The secondary structure topology consists of 11 α-helices and 17 β-strands. The FAD-binding domain (denoted by F) is characterized by 6 α-helices and 10 β-strands whereas the interface domain (denoted by I) comprises 5 α-helices and 7 β-strands. Overall the structure is analogous to that of pkDAO[18, 25] and RgDAO[27].

When the head region of chDAO is compared to pkDAO there are 3 additional α-helices (αI1a and αI1b between βI1 and βI2 and αI3a after αI3) and β-strands (βF3a after βF3 and βI7a and βI7b after βI7) (Fig. 3). However, RgDAO contains one more β-strand than chDAO. Two main topological differences are also observed between chDAO and pkDAO as well as RgDAO. One is the presence of shorter active site loop (9 residues in chDAO versus 13 in pkDAO) connecting βI6 and βI7 in chDAO (Fig. 3). This active site loop connects βI5 and βI6 in pkDAO, but this type of loop is absent in RgDAO. Another is the absence of a long C-terminal loop found in RgDAO (6 residues in chDAO and 4 in pkDAO versus 21 in RgDAO). This C-terminal loop connects βF5 and βF6 in each DAO (Fig. 3). The active site loop found in pkDAO, proposed by Mattevi et al[25], acts as a 'lid' controlling the access of substrate to the active site.
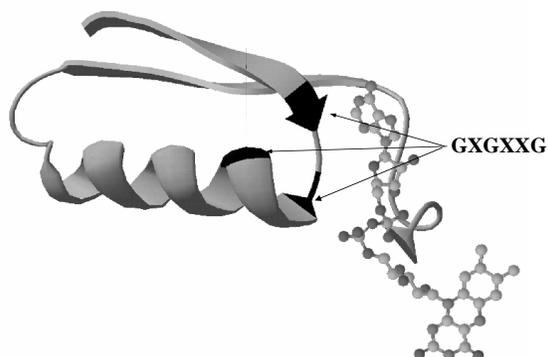
Mode of dimerization

Native DAOs from microbial and mammalian sources form a dimer composed of identical subunits[25, 27]. Each monomer contains one non-covalently bound
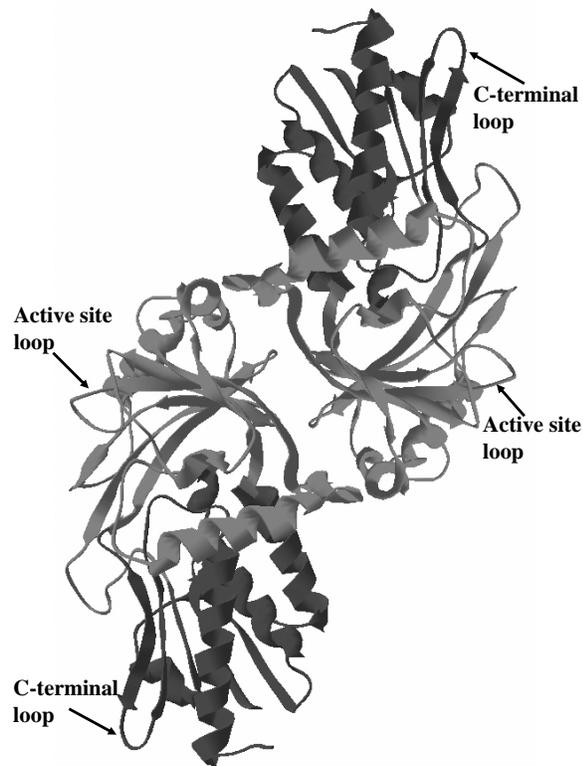
Fig. 4 The DAO 'head-to-head' dimer viewed along the two-fold axis.

FAD[28]. chDAO shows a theoretical 'head-to-head' interaction of the subunits, resulting in an elongated dimer of cylindrical shape (Fig. 4). The same mode of dimerization has also been reported in pkDAO by Mattevi et al[25]. For RgDAO, a different mode of dimerization has been proposed in which a 'head-to-tail' interaction between the two monomers yields a spherical dimer. The buried surface area in RgDAO is much wider than that observed in the 'head-to-head' dimer of pkDAO[29]. Another striking difference between mammalian and yeast DAOs is the presence of a long C-terminal loop in RgDAO, not present in other known DAO sequences. This loop is responsible for making the 'head-to-tail' mode of dimerization that gives the dimer wider interaction between two monomers. The 'head-to-tail' mode dimer thereby provides a more stable state and a tighter binding of FAD than the 'head-to-head' mode dimer found in mammalian and carp DAOs. The three-dimensional structures of DAOs reveal that evolutionary pressure has led to the conformational change from microbial to mammalian DAOs. These DAOs share the same chemical process with different catalytic efficiency,

Fig. 5 The FAD-binding site of chDAO showing the typical βαβ motif for a dinucleotide-binding site. The α-helix is connected with the β-strands by the loops, Gly residues are indicated by the arrows and FAD in balls and sticks.

stability, and mode of dimerization. This is supported by limited proteolysis studies; this loop can be easily cleaved off yielding a monomeric RgDAO form[30].

FAD-binding motif

The N-terminal amino acid sequence of chDAO reveals a high degree of homology with those of DAOs previously reported[12,31–33]. The N-terminal sequence includes the highly conserved region I of DAOs[31], which contain the GXGXXG motif required for binding of FAD[32]. chDAO contains the conserved consensus Rossman fold[34] in which a βαβ motif is common for FAD and NAD(P)H-dependent oxidoreductases[35,36] (Fig. 5). pkDAO and RgDAO also show the same βαβ motif. The central part of this consensus motif is a sequence GXGXXG close to the N-terminus. The importance of the glycine residues in the conserved GXGXXG is well understood[37]; the first strictly conserved glycine allows for a tight turn of the main chain, which is important for positioning the second glycine. The second glycine, because of its missing side chain, permits close contact of the main chain to the pyrophosphate of FAD. The third glycine allows the helix to closely pack with the β-sheet. On the basis of structural and sequence homologies[37,38], chDAO can be classified as a member of a large glutathione reductase (GR) family in which all the family members adopt the Rossmann fold[37,38], and therein into a subgroup GR$_2$ which is reported to show sequence similarity mainly within 30 residues in the N-terminal region.

Active site cavity

In the active site cavity only three catalytic residues named Tyr224, Tyr228, and Arg283, have been found
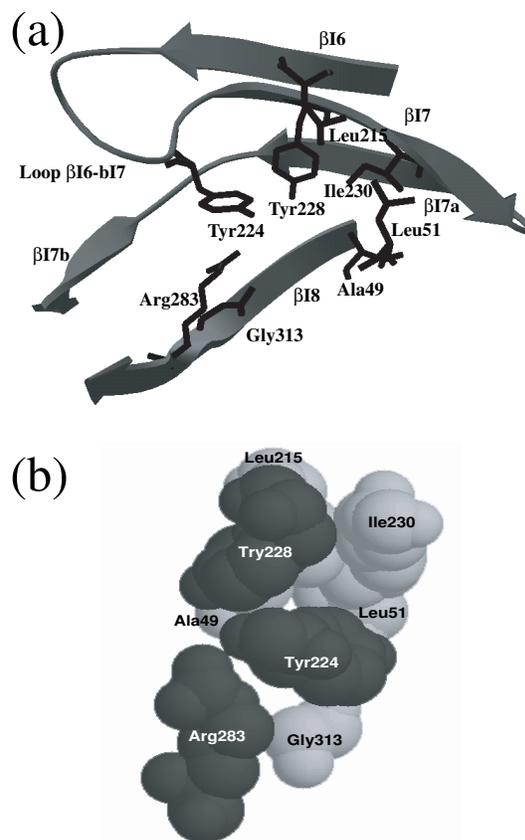
Fig. 6 (a) Active site cavity of chDAO containing key catalytic residues Tyr224, Tyr228, and Arg283 is surrounded by hydrophobic side chains of Ala49, Leu51, Leu215, Ile230, and Gly313. (b) Space-filling model of chDAO active site cavity. Catalytic residues are in black and hydrophobic residues in grey.

in pkDAO[25,39]. These three residues were also found in a similar conformation in chDAO and active site cavity is delimited by four β-strands βI7, βI7a, βI7b, and βI8 (Fig. 6). Interestingly, a larger loop (216-228) found in pkDAO and a shorter one (218-226) in chDAO, which Mattevi et al[23] proposed to act as a 'lid' controlling the access to the active site, is absent in RgDAO[27,39]. The conformational change in the large active site loop determines the overall rate of turnover of DAOs. It makes the turnover of mammalian DAOs comparatively slow, as the product release becomes the rate-limiting step[37]. The active site loop contains an important residue Tyr224 which is also conserved in chDAO[12]. Tyr224 is probably involved in a broad range of substrates/products fixation and interacts with substrate α-amino group and an active site water molecule[40] (Fig. 6). The

carboxylate group of the substrate makes a strong hydrogen bond with the OH of Tyr228 and a salt bridge with Arg283[25, 39]. The substrate is surrounded by several hydrophobic side chain residues delimiting the active site (that of Ala49, Leu51, Leu215, Ile230, and Gly313) (Fig. 6). In RgDAO, the Tyr238 side-chain is placed at a similar position, but in a different segment[39]. A corresponding loop that could exert the same function is not present in yeast DAO. However, Tyr238 appears to play a comparable role in a rudimentary fashion. The side-chain of this amino acid is assumed to take the open conformation in the uncomplexed enzyme, and this might initiate an interaction with the substrate, leading it into the bottom of the active site. The side chain of Tyr238 takes the open conformation in the free enzyme, initiates an interaction with substrate, and leads it into the active site. This scenario explains the higher turnover rate of RgDAO[39]. The shorter active site loop found in chDAO might be responsible for the low K_m values for D-alanine and the higher turnover rate of chDAO compared to that of pkDAO. The apparent K_m value of chDAO for D-alanine (0.23 mM) was lower than that of mammalian and yeast DAOs[41–44]. chDAO has a catalytic constant of about 190 s^{-1} compared to 10 s^{-1} for pkDAO and 300 s^{-1} for RgDAO[3, 43, 45], indicating a much higher turnover rate of chDAO compared to that of pkDAO.

Indeed, fully automated sequence alignment algorithms often misplace insertions and deletions when the overall sequence identity level falls below 40%. The accuracy of a model is essentially limited by the deviation of the template structure used relative to the experimental control structure. This limitation is inherent to the methods used, since the model results from an extrapolation. As a consequence, the core C_α atoms of a protein which share 35%–50% sequence identity with their templates will generally deviate by 1.0–1.5 Å from their counterparts having experimentally elucidated structures[46]. chDAO showed a less than 1.0 Å deviation of C_α atoms compared to their experimental structure because it shares 60% sequence identity with the modelling templates (pkDAO).

REFERENCES

1. Dunlop DS, Neidle A, McHale D, Dunlop DM, Lajtha A (1986) The presence of free D-aspartic acid in rodents and man. *Biochem Biophys Res Comm* **141**, 27–32.

2. Hashimoto A, Nishikawa T, Hayashi T, Fujii N, Harada K, Oka T, et al (1992) The presence of free D-serine in rat brain. *FEBS Lett* **296**, 33–6.

3. Sarower MG, Okada S, Abe H (2005) Catalytic and structural characteristics of carp hepatopancreas D-amino acid oxidase expressed in *Escherichia coli*. *Comp Biochem Physiol* **140B**, 417–25.

4. Sentheshanmuganathan S, Nickerson WJ (1962) Transaminase and D-amino acid oxidase of *Trigonopsis variabilis*. *J Gen Microbiol* **27**, 465–71.

5. Kawamoto S, Kobayashi M, Tanaka Fukui S (1977) Production of D-amino acid oxidase by *Candida tropicalis*. *J Ferment Tech* **55**, 13–8.

6. Simonetta MP, Vanoni MA, Curti B (1982) D-Amino acid oxidase activity in the yeast *Rhodotorula gracilis*. *FEMS Microbiol Lett* **15**, 27–31.

7. Konno R, Yasumura Y (1992) D-Amino acid oxidase and its physiological function. *Int J Biochem* **24**, 519–24.

8. Sarower MG, Matsui T, Abe H (2003) Distribution and characteristics of D-amino acid and D-aspartate oxidases in fish tissues. *J Exp Zool* **295**, 151–9.

9. Sarower MG, Matsui T, Abe H (2004) Distribution and substrate specificity of D-amino acid and D-aspartate oxidases in marine invertebrates. *Sci Asia* **30**, 335–40.

10. de Duve Baudhuin P (1966) Peroxisomes (microbodies and related particles). *Physiol Rev* **46**, 323–57.

11. Krebs HA (1935) Metabolism of amino acids. III. Determination of amino acids. *Biochem J* **29**, 1620–44.

12. Ronchi S, Minchiotti L, Galliano M, Curti B (1982) The primary structure of D-amino acid oxidase from pig kidney. *J Biol Chem* **257**, 8824–34.

13. Fukui K, Watanabe F, Shibata T, Miyaki Y (1987) Molecular cloning and sequence analysis of cDNAs encoding porcine kidney D-amino acid oxidase. *Biochemistry* **26**, 3612–8.

14. Sarower MG, Okada S, Abe H (2003) Molecular characterization of D-amino acid oxidase from common carp *Cyprinus carpio* and its induction with exogenous free D-alanine. *Arch Biochem Biophys* **420**, 121–9.

15. Horiike K, Tojo H, Arai R, Nozaki M, Maeda T (1994) D-Amino acid oxidase is confined to the lower brain stem and cerebellum in rat brain: regional differentiation of astrocytes. *Brain Res* **652**, 297–303.

16. Schell MJ, Molliver ME, Synder SH (1995) D-Serine, an endogenous synaptic modulator: Localization to astrocytes and glutamate-stimulated release. *Proc Natl Acad Sci USA* **92**, 3948–52.

17. D'Aniello A, D'Onofrio G, Pischetola M, D'Aniello G, Vetere A, Petrucelli L, Fisher GH (1993) Biological role of D-amino acid oxidase and D-aspartate oxidase. *J Biol Chem* **268**, 26941–9.

18. Mizutani H, Miyahara I, Hirotsu K, Nishina Y, Shiga K, Setoyama C, Miura R (1996) Three-dimensional structure of porcine kidney D-amino acid oxidase at

3.0 Å resolution. *J Biochem* **120**, 14–7.

19. Huang X, Miller W (1991) A time-efficient, linear-space local similarity algorithm. *Adv Appl Math* **12**, 337–57.

20. Peitsch MC (1996) ProMod and Swiss-model: Internet-based tools for automated comparative protein modeling. *Biochem Soc Trans* **24**, 274–9.

21. Mizutani H, Miyahara I, Hirotsu K, Nishina Y, Shiga K, Setoyama C, Miura R (2000) Three-dimensional structure of the purple intermediate of porcine kidney D-amino acid oxidase. Optimization of the oxidative half-reaction through alignment of the product with reduced flavin. *J Biochem* **128**, 73–81.

22. Miura R, Setoyama C, Nishina Y, Shiga K, Mizutani H, Miyahara I, Hirotsu K (1997) Structural and mechanistic studies on D-amino acid oxidase-substrate complex: Implications of the crystal structure of enzyme-substrate analog complex. *J Biochem* **122**, 825–33.

23. van Gunsteren WF, Billeter SR, Eising AA, Hünenberger PH, Krüger P, Mark AE, Scott WRP, Tironi IG (1996) Biomolecular Simulations: The GROMOS96 Manual and User Guide. VdF Hochschulverlag ETHZ, Zurich, Switzerland.

24. Guex N, Peitsch MC (1997) SWISS-MODEL and the Swiss-PdbViewer: an environment for comparative protein modeling. *Electrophoresis* **18**, 2714–23.

25. Mattevi A, Vanoni MA, Todone Rizzi M, Teplyakov A, Coda A, Bolognesi M, Curti B (1996) Crystal structure of D-amino acid oxidase: a case of active site mirror-image convergent evolution with flavocytochrome b_2. *Proc Natl Acad Sci USA* **93**, 7496–501.

26. Wierenga RK, Drenth J, Schulz GE (1983) Comparison of three dimensional protein and nucleotide structure of the FAD-binding domain of *p*-hydroxybenzoate hydroxylase with the FAD as well as NADPH-binding domain of glutathion reductase. *J Mol Biol* **167**, 725–39.

27. Pollegioni L, Diederichs K, Molla1 G, Umhau S, Welte W, Ghisla S, Pilone Simmonetta M (2002) Yeast D-amino acid oxidase: structural basis of its catalytic properties. *J Mol Biol* **324**, 535–46.

28. Pilone Simonetta M, Pollegioni L, Casalin P, Curti B, Ronchi S (1989) Properties of D-amino acid oxidase from *Rhodotorula gracilis*. *Eur J Biochem* **180**, 199–204.

29. Umhau S, Diederichs K, Welte W, Ghisla S, Pollegioni L, Molla G, Porrini D, Simonetta Pilone M (1999) Very high resoution crystal structure of D-amino acid oxidase. Insights into the reaction mechanisms and mode of ligand binding. In: Ghisla S, Kroneck P, Acheroux P, Sund H (eds) *Flavins and Flavoproteins*, Weber, Berlin, pp 567–70.

30. Pollegioni L, Ceciliani F, Curti B, Ronchi S, Pilone MS (1995) Studies on the structural and functional aspects of *Rhodotorula gracilis* D-amino acid oxidase by limited proteolysis. *Biochem J* **310**, 577–83.

31. Faotto L, Pollegioni L, Ceciliani F, Ronchi S, Pilone MS (1995) The primary structure of D-amino acid oxidase from *Rhodotorula gracilis*. *Biotechnol Lett* **17**, 193–8.

32. Komatsu K, Matsuda A, Sugiura K (1987) Gene of D-amino acid oxidase. Japan Patent. 1987262994-A/1.

33. Isogai T, Ono T, IshitaniY, Kojo H, Ueda Y, Kohsaka M (1990) Structure and expression of cDNA for D-amino acid oxidase active against cephalosporin C from *Fusarium solani*. *J Biochem* **108**, 1063–9.

34. Rossmann MG, Moras D, Olsen KW (1974) Chemical and biological evolution of nucleotide binding proteins. *Nature* **250**, 194–9.

35. Fraaije MW, Mattevi A (2000) Flavoenzymes: diverse catalysts with recurrent features. *Trends Biochem Sci* **25**, 126–32.

36. Dyn O, Eisenberg D (2001) Sequence-structure analysis of FAD-containing proteins. *Protein Sci* **10**, 1712–28.

37. Wierenga RK, Terpstra P, Hol WG (1986) Prediction of the occurrence of the ADP-binding βαβ-fold in proteins, using an amino acid sequence fingerprint. *J Mol Biol* **187**, 101–7.

38. Macheroux P, Seth O, Bollschweiler C, Schwarz M, Kurfürst M, Au LC, Ghisla S (2001) L-Amino-acid oxidase from the Malayan pit viper *Calloselasma rhodostoma* - Comparative sequence analysis and charaterization of active and inactive forms of the enzyme. *Eur J Biochem* **268**, 1679–86.

39. Todone F, Vanoni MA, Mozzarelli A, Bolognesi M, Coda A, Curti B, Mattevi A (1997) Active site plasticity in D-amino acid oxidase: a crystallographic analysis. *Biochemistry* **36**, 5853–60.

40. Pollegioni L, Fukui K, Massey V (1994) Studies on the kinetic mechanism of pig kidney D-amino acid oxidase by site-directed mutagenesis of tyrosine 224 and tyrosine 228. *J Biol Chem* **269**, 31666–73.

41. Kishore G, Vaidyanathan CS (1976) Purification and properties of D-amino acid oxidase of *Aspergillus niger*. *Indian J Biochem* **13**, 216–22.

42. Pilone MS, Vanoni MA, Casalin P (1987) Purification and properties of D-amino acid oxidase, an inducible flavoenzyme from *Rhodotorula gracilis*. *Biochim Biophys Acta* **914**, 136–42.

43. Pollegioni L, Langkau B, Tischer W, Ghisla S, Pilone MS (1993) Kinetic mechanism of D-amino acid oxidase from *Rhodotorula gracilis* and *Trigonopsis variabilis*. *J Biol Chem* **268**, 13850–7.

44. Yurimoto H, Hasegawa T, Sakai Y, Kato N (2001) Characterization and high-level production of D-amino acid oxidase in *Candida boidinii*. *Biosci Biotechnol Biochem* **65**, 627–33.

45. Pörter DJT, Voet JG, Bright HJ (1977) Mechanistic features of the D-amino acid oxidase reaction studied by double stopped flow spectrophotometry. *J Biol Chem* **252**, 4464–73.

46. Chothia C, Lesk AM (1986) The relation between the divergence of sequence and structure of proteins. *EMBO J* **5**, 823–6.